



## 15 **Abstract**

16 In this work, we examined the effects of albedo and solar flux on climate parameters in Burkina Faso.  
17 Our study shows a continued decrease in albedo, leading to an increase in temperature, humidity and  
18 precipitation. These climatic conditions can increase the risks of prolonged droughts and floods. This  
19 drop in albedo is linked to solar activity, growing urbanization, deforestation and global climate change.  
20 Low solar activity and solar high-speed flows caused by regions of corotative interactions lead to heavy  
21 precipitation. The use of reflective construction materials, i.e. high albedo, in urban infrastructure and  
22 stopping the transformation of forests into cultivable land can contribute to mitigating the diminution in  
23 albedo and consequently global warming.

24 **Keywords** : Albedo, Solar flux, Temperature, Precipitation, Solar Activity, Climate, Burkina Faso

## 25 **1. Introduction**

26 The Sun is the main source of energy, through its electromagnetic radiation which heats the earth's  
27 atmosphere and determines meteorological processes. Albedo is the ability of surfaces to reflect sunlight  
28 (heat from the sun). Clear surfaces reflect a large part of the sun's rays towards the atmosphere (high  
29 albedo). Dark surfaces absorb the sun's rays (low albedo). Albedo is measured on a scale of 0 to 1.  
30 Albedo value 0 indicates that all light is absorbed by the surface and is not reflected and value 1 indicates  
31 that all light is reflected by the surface and there is no absorption. Although only one of many factors  
32 contributing to climate change, surface albedo is an important parameter in the energy balance of the  
33 land cover and is considered an essential climate variable. Variations in surface albedo can be used as  
34 a diagnostic tool for local climate change according to authors such as [1]; [2]. Climate change is defined  
35 as general changes in climate over time. This includes global warming, more frequent and intense  
36 extreme weather events (like hurricanes and monsoons), and bizarre weather conditions. A change in  
37 albedo or a change in global temperatures can create a feedback loop between the two. The Earth's  
38 albedo has been declining for decades, contributing to global warming. Local/regional climate change  
39 caused by deforestation and land use changes is synergistic with global warming, causing a more  
40 dynamic climate change process [3]. The temporal and spatial variation of albedo has been closely  
41 related to global climate change as well as regional weather and environment [4]; [5]. [6] found a strong  
42 inverse exponential relationship with a correlation ( $r = 0.95$ ) between satellite-observed albedo and  
43 precipitation. Similar relationships have been discovered in West Africa between albedo and  
44 precipitation by several researchers [7]; [8]; [9]. [10] showed the existence of a negative correlation  
45 between albedo and land surface temperature, with  $R^2 = -0.6109$ . [11] Showed that albedo influences  
46 surface temperature. [12] showed that higher rainfall is associated with lower albedos. [13] Showed that  
47 flooding caused by heavy precipitation in Canada tends to follow the arrival of high-speed solar wind  
48 streams from coronal holes. [14] have shown the possible role of solar activity on climate change. The  
49 objective of this work is to analyze the impact of changes in albedo and solar flux on climatic parameters  
50 in Burkina Faso. More precisely the effect of albedo and solar flux in three areas of Burkina Faso with  
51 different plant covers. Burkina Faso is subdivided into three large climatic zones (Fig.1): the Sahelian  
52 zone in the north with precipitation less than 600 millimeters per year (mm/year), the Sudano-Sahelian

53 region on a savannah plateau with precipitation of 600 to 900 millimeters per year (mm/year) and slightly  
 54 cooler temperatures, and the wetter southern Sudanian zone with average precipitation between 900  
 55 and 1,200 mm/year.

56

57 **2. Data and Methodology**

58 In this work, we used albedo, precipitation, temperature and specific humidity, available at  
 59 <https://power.larc.nasa.gov/data-access-viewer/>. The solar wind speed available on the site  
 60 <https://omniweb.gsfc.nasa.gov/form/dx1.html> was used to calculate the energy carried by the solar wind  
 61 using the formula:

62 
$$E_{sw} = \frac{1}{2} \rho_{sw} V_{sw}^3$$

63  $\rho_{sw} = 1408 \text{ kg/m}^3$  and represents the density of the solar wind.

64 We have also used the sunspot number available on the site <http://www.sidc.be/silso/>. Hourly cosmic  
 65 ray data were obtained from the Thule Neutron Monitoring Station (76.5°N, 68.5°W, 26.0 m) with a  
 66 geomagnetic cut-off rigidity of 1.0 GV. Then we calculated the annual averages of cosmic rays.

67 These data were used to analyze the impact of albedo and solar flux on climate parameters in three  
 68 cities in Burkina Faso, namely Bobo-Dioulasso (latitude=11.149; longitude=-4.242), Ouagadougou  
 69 (latitude=12.365; longitude=-1.507) and Dori (latitude=14.007; longitude=-0.073). These three cities are  
 70 located in different climatic zones (figure 1) of Burkina Faso.



71

72 Figure 1: Climatic zones of Burkina Faso

73 **3. Results and discussion**

74 From figures 2 to 7, the relationship between albedo, solar flux and climatic parameters in Burkina Faso  
 75 is investigated for the period 1984-2022.

76 Figure 2, presents the precipitation and albedo profiles in three cities Bobo Dioulasso, Ouagadougou  
77 and Dori during the period 1984 to 2022. In Figure 2.a, we observe a decrease in surface albedo from  
78 1984 to 1990. During this period, we recorded a drop in precipitation. From 1990 to 1999 we observe a  
79 constant evolution of the albedo then a slight increase in the albedo. During this period, we observe a  
80 fluctuation in precipitation, but we can notice an increase in maximum amplitudes. During the period  
81 2000 to 2001, a strong decrease in albedo is observed. The albedo drops from 0.2 to 0.16. Then we  
82 observe a strong fluctuation and continuous decrease in albedo until 2022. During this period we also  
83 record a strong fluctuation in precipitation; but we can also notice a continuous increase in the maximum  
84 amplitudes of precipitation. The highest rainfall is recorded in 1998 (1223.44 mm), 2010 (1244.53 mm)  
85 2019 (1455.47 mm) and 2021 (1288 mm).

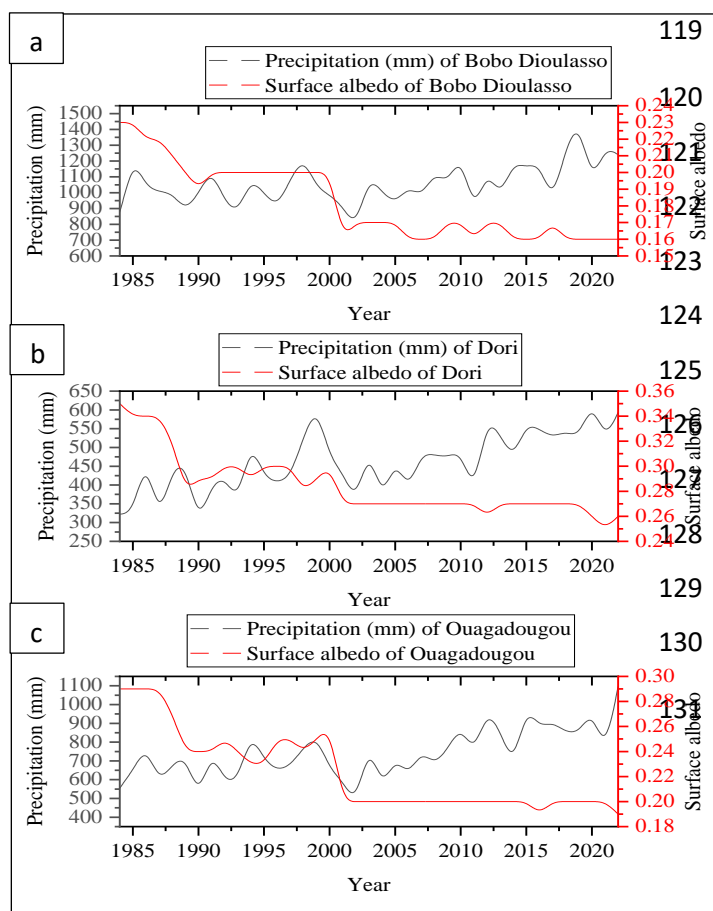
86 In Figure 2.b, we observe a decrease in albedo from 1984 to 1989 and a stable evolution of maxima  
87 amplitude of the precipitation. A fluctuation in albedo is observed from 1989 to 2000 with an increase in  
88 maximum precipitation amplitudes. From 2000 to 2001 a sudden decrease in albedo is observed and a  
89 drop in precipitation is also observed. From 2001 until 2022, a linear and constant evolution of the albedo  
90 is observed, except 2012 and 2021 which records a slight fluctuation. The year 2021 records the lowest  
91 albedo during our study period. During the period 2001 to 2022, a strong fluctuation in precipitation is  
92 observed; but overall we remark an increase in the maximum amplitudes of precipitations. The lowest  
93 precipitation was observed in 1987 (305.86 mm) and 1990 (295.31 mm).

94 In Figure 2.c, we observe a constant evolution of the albedo from 1984 to 1987 before gradually  
95 decreasing from 1987 to 1989. During this period we observe a decrease in the maximum amplitudes  
96 of precipitations. From 1989 to 2000 we observe a strong fluctuation in albedo. During this period an  
97 increase in maximum precipitation is observed. From 2000 to 2001, the albedo drops sharply, leading  
98 to a sudden decrease in precipitation until 2002. Then from 2001 to 2022, a linear and constant evolution  
99 of the albedo is observed with slight variations in 2016 and 2022. During this period there is a strong  
100 fluctuation in precipitation with an increase in maximum amplitudes. The lowest precipitation is recorded  
101 in 1983 (442.97 mm), 1990 (500.98 mm) and 2002 (469.34 mm) and the highest precipitation is recorded  
102 in 2012 (970.31 mm), in 2015 (986.13 mm), 2020 (970.31 mm) and 2022 (1096.92 mm)

103 Figure 3, presents the temperature and albedo profiles of Bobo Dioulasso, Ouagadougou and Dori  
104 during the period 1984 to 2022. In Figure 3.a, we observe a decrease in albedo from 1984 to 1990; from  
105 1991 to 2000 a linear and constant evolution of the albedo is observed. During these periods we observe  
106 a decrease in the earth's temperature from 1984 to 1985 then increases slightly from 1985 to 1987  
107 before fluctuating slightly around 27°C to 28°C from 1987 to 2000. Then the albedo drops sharply from  
108 2000 to 2001. During this period the temperature increased sharply and recorded the highest  
109 temperature in 2002 (29.06 °C) during our study period. Then a slight fluctuation in albedo followed by  
110 a weak fluctuation in temperature around 27°C to 28°C. The lowest temperature was recorded in 1986  
111 (26.63°C).

112 In Figure 3.b, we observe a continuous decrease in the albedo from 1984 to 1989. During this period,  
113 we observe an increase in temperature with a peak in 1987 (30.01 °C) before decreasing until 'in 1989.  
114 From 1989 to 2000 we observe a weak fluctuation in the albedo and during this period, the largest peak  
115 in temperature is observed in 1990 (30.3 °C) before gradually decreasing until 1999. From 2000 the

116 albedo drops sharply until 2001, then a linear and constant evolution is observed until 2022, with slight  
 117 fluctuations in 2012 and 2021. During this period heat waves are observed, with the largest heat peak  
 118 recorded in 2004 (30.42 °C).



132

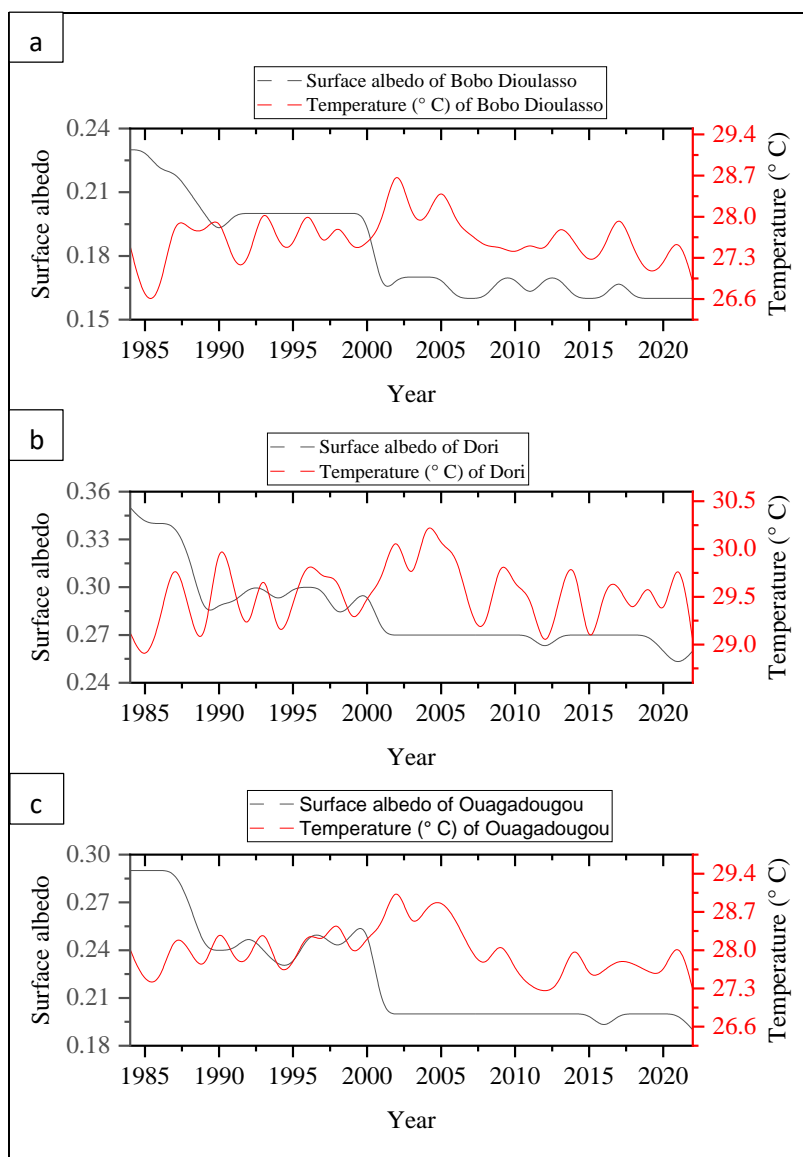
133

Figure 2: Precipitation and albedo profile during the period 1984-2022

134 In Figure 3.c, we observe a linear and constant evolution of the albedo from 1984 to 1987. During this  
 135 period a decrease in temperature is observed from 1984 to 1986. A decrease in the albedo is observed  
 136 from 1987 to 1989 and an albedo fluctuation around 0.23 to 0.26 from 1990 to 2000. During these  
 137 periods, a weak temperature fluctuation around 27 °C and 28 °C is observed. A sudden decrease in  
 138 albedo was recorded from 2000 to 2001 and led to a sharp increase in temperature. The highest  
 139 temperature was recorded in 2002 (29.37°C) during our period covered by our study.

140 Figure 4, presents the temporal evolution curves of the annual averages of precipitation and specific  
 141 humidity in the cities of Bobo Dioulasso, Ouagadougou and Dori during the period 1984 to 2022. The  
 142 specific humidity (absolute) is the actual amount of moisture in the form of water vapor in the air. Specific  
 143 humidity is measured in grams of water vapor per kilogram of air (g/kg). The two parameters studied  
 144 present a good correlation. The correlation is 0.72 for the city of Bobo Dioulasso, 0.76 for the city of  
 145 Ouagadougou and 0.69 for the city of Dori. The highest precipitation coincides with the highest specific  
 146 humidity. Also the lowest precipitation coincides with the lowest specific humidity. We also observe an  
 147 increase in the maximum amplitudes of precipitation and specific humidity from 2001 to 2022. In Figure  
 148 4.a, the lowest specific humidity and the lowest precipitation is recorded in 2002 (11.11 g/kg;

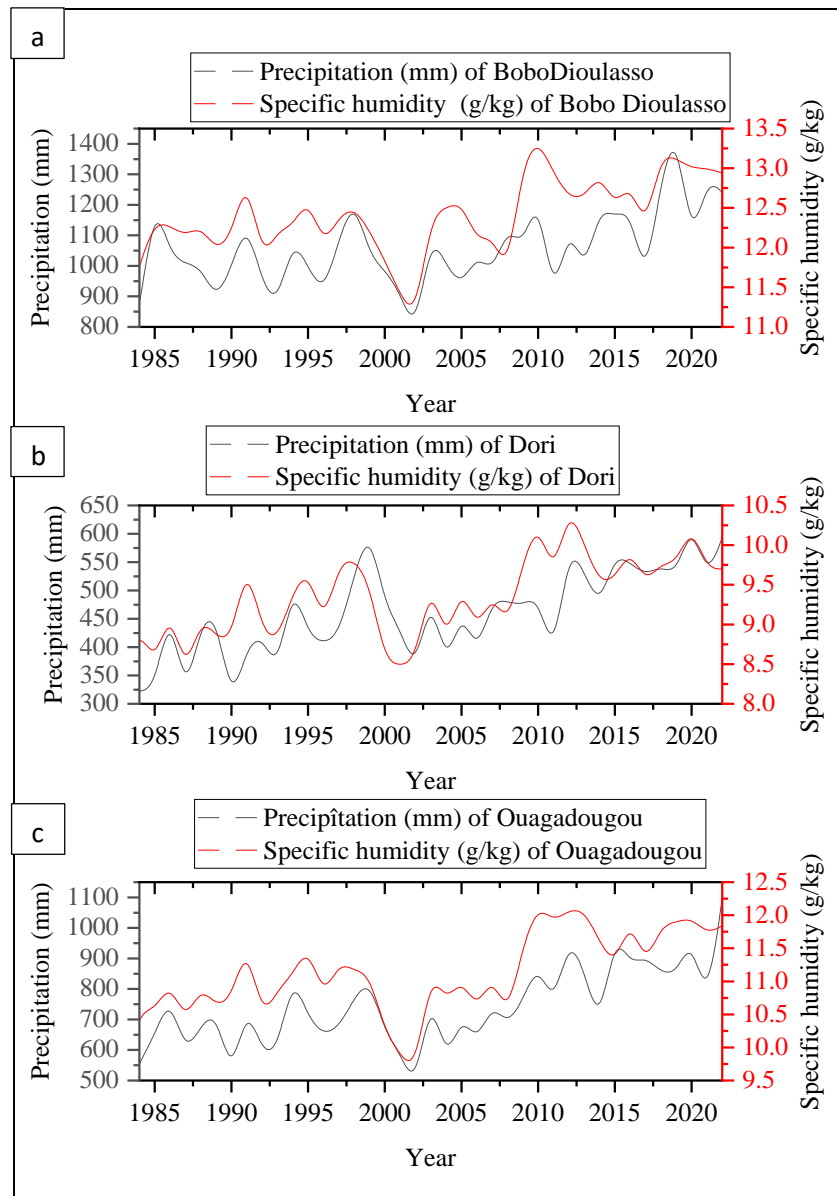
149 775.52mm). The highest specific humidity and precipitation are recorded in 2010 (13.37 g/kg; 1244.53  
 150 mm) and in 2019 (13.12 g/kg; 1455.47 mm). In Figure 4.b, the lowest specific humidity is recorded in  
 151 1984 (8.42 g/kg), in 1987 (8.36 g/kg), in 2000 (8.54 g/kg) and in 2001 (8.48 g/kg) and the lowest  
 152 precipitation is observed in 1987 (305.86 mm) and 1990 (295.31 mm). The highest specific humidity  
 153 was observed in 2010 (10.31 g/kg), in 2012 (10.5 g/kg) and the highest precipitation was recorded in  
 154 1999 (611.72 mm), in 2012 (580 .08 mm) in 2015 (564.26 mm) and 2020 (622.27 mm). In Figure 4.c,  
 155 the lowest specific humidity and precipitation are observed in 1983 (9.64 g/kg; 442.97 mm) and in 2002  
 156 (9.64 g/kg; 469.34 mm). High specific humidity and precipitation are observed in 2010 (12.15 g/kg;  
 157 885.94 mm) in 2012 (12.08 g/kg; 970.31 mm) in 2022 (11.84 g/kg; 1096. 92mm). These observations  
 158 show that high specific humidity leads to heavy precipitation.



159

160

Figure 3: Surface temperature and albedo profile during the period 1984-2022



161

162

Figure 4: Profile of precipitation and specific humidity during the period 1984-2022.

163

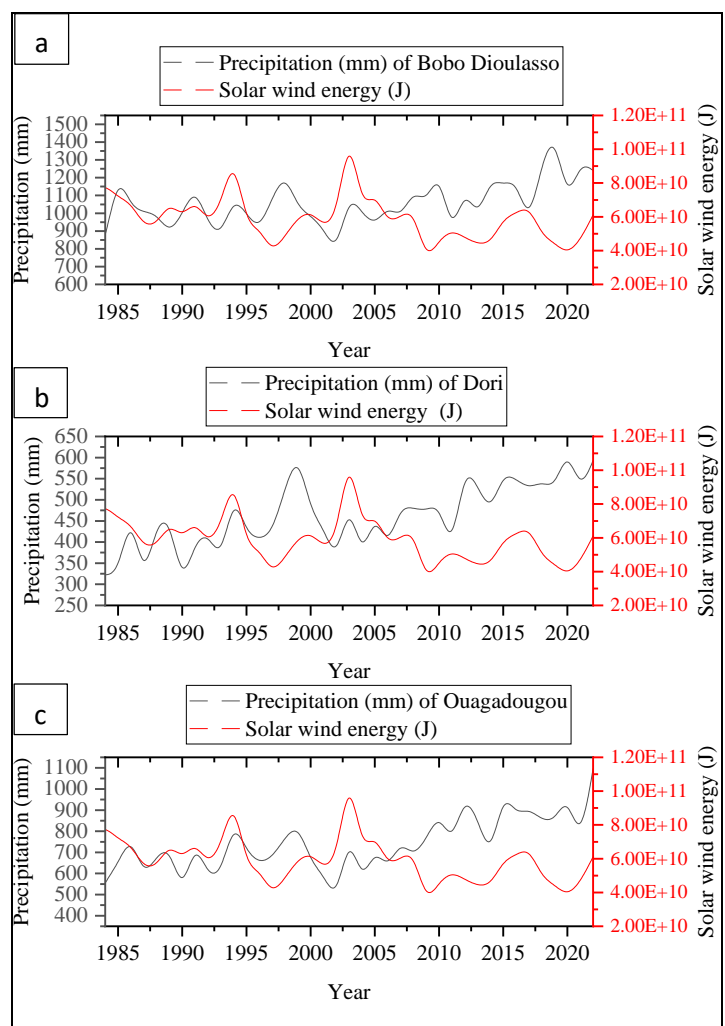
Through the analysis of figures 2, 3 and 4 we can see that the quantity of precipitation varies greatly depending on the specific humidity, which varies with the temperature. Indeed, as the temperature increases, the air is able to retain more and more humidity. We are more likely to receive rain when humidity is higher because water vapor expands more quickly. This is based on the Clausius-Clapeyron (CC) relationship which states that as temperature increases, the atmosphere has the capacity to retain more moisture, at a rate of 6% to 7% °C<sup>-1</sup> [15]. Thus, extreme precipitation scales with surface water or the water column [16], [17], so we can expect extreme precipitation to increase with temperature increase. We also observed that a continued decrease in albedo leads to heat waves. Indeed, the reduction in albedo leads to an increase in the absorption of solar radiation by the ground and therefore the transfer of sensible and latent heat to the atmosphere. This produces higher global warming. These observations are in agreement with the work of [10] which showed the existence of a negative correlation between albedo and land surface temperature, with  $R^2 = -0.6109$ . Also, [11] showed that albedo influences surface temperature. The decrease in albedo contributes to the increase in convective clouds,

175

176 and therefore precipitation. This global warming and increased precipitation causes the evaporation of  
177 a greater quantity of water, therefore high specific humidity, which can lead to more intense droughts  
178 and a higher risk of flooding. Overall, weird weather conditions. These observations show that a change  
179 in albedo influences climatic parameters (temperature, specific humidity and precipitation). These  
180 observations are in agreement with the work of [12] who found higher rainfall at lowers albedos. We also  
181 note that the amplitude of precipitation and specific humidity is important in Bobo Dioulasso compared  
182 to Ouagadougou and similarly the amplitude of precipitation and specific humidity is important in  
183 Ouagadougou compared to Dori. The amplitude of temperature and albedo are significant in the town  
184 of Dori compared to Ouagadougou and Ouagadougou compared to Bobo-Dioulasso. However, a  
185 continuous decrease in albedo is observed in all three cities. This is explained on the one hand by the  
186 difference in plant cover and the quantity of water in the soil in these different zones. On the other hand,  
187 Burkina Faso knows an increase in population in recent decades as well as rapid urbanization and  
188 industrialization concentrated in large cities. This caused a great revolution in land use. This revolution  
189 is accompanied by a significant thermal change, creating a thermal imbalance between urban and rural  
190 areas. This series of extreme heat waves increases cooling energy consumption in buildings,  
191 deteriorates air quality and affects people's health [18], leading to an increase in health and mortality  
192 [19]; [20], [21]; [22]. Possible symptoms caused by heat stress include swelling, rashes, and heat stroke  
193 related to neurological disorders when body temperature reaches 40.6°C [23]. Thus, strategies must be  
194 implemented to reduce the conditions of global warming in Burkina Faso. Several studies have shown  
195 a direct link between high urban temperatures and the lack of vegetation, highlighting the potential of  
196 vegetation to reduce extreme temperatures, especially during the hot season, through two effects:  
197 evapotranspiration and shading [24]; [25]. Deforestation can decrease evapotranspiration and increase  
198 surface temperatures by 3° to 5°C [26]. [27] through deforestation simulation studies have shown either  
199 a decrease in precipitation due to the weakening of precipitation recycling, or an increase in precipitation  
200 due to the intensification of convection over areas heterogeneity of the earth's surface. For [28],  
201 urbanization can potentially have a global warming effect by reducing the Earth's albedo. Tropical forests  
202 are increasingly recognized as major resources for mitigating climate change [29]. The work of [2]  
203 showed that reducing deforestation of all forest types, converting annual or grassland agriculture to  
204 perennial agriculture, and properly selecting greenhouse covers for new protected agricultural systems  
205 could help mitigate climate change regional. According to the work of [10]; [28], green roofs have a  
206 higher albedo than many conventional black/brown roofs. The albedo of urban land is 0.01–0.02 lower  
207 than that of adjacent cultivated land [30]. The albedo of urban land can be regulated and improved by  
208 using more reflective materials and also by reducing deforestation.

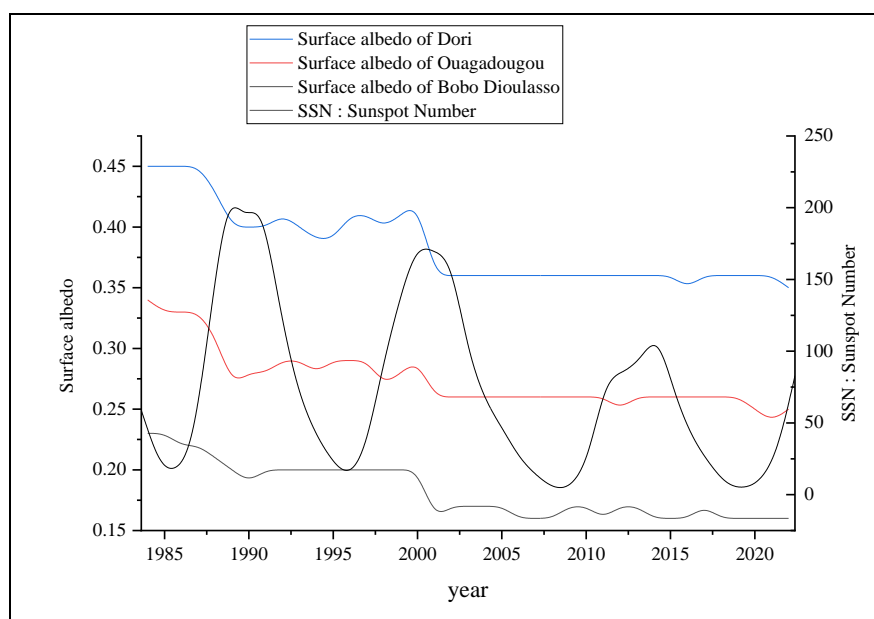
209 Figure 5 presents the profile of the solar wind energy and precipitation of Bobo-Dioulasso, Ouagadougou  
210 and Dori during the period 1984 to 2022. In Figures 5.a, 5.b and 5.c, the two parameters studied present  
211 a weak correlation. However, we can observe some peaks in the solar wind energy to coincide with  
212 heavy annual precipitation. This can be clearly observed in 1994 and 2003 which correspond to periods  
213 of the descending phases of solar cycles 22 and 23. Heavy precipitation is also observed when weak  
214 solar wind energy are recorded. These periods coincide with the solar minimum of solar cycles, which  
215 are dominated by slow solar winds [31], [32]. Exceptionally, we generally observe a drop in the amplitude

216 of the solar wind energy after the long solar minimum which preceded solar cycle 23 (2008-2022). During  
 217 this period, there is an increase in precipitation. These observations are in agreement with the work of  
 218 [14] who found that precipitation is important at solar minimum where quiet activity is dominant.  
 219 According to the work of [33], [34], solar cycle 24 at has knows a lower solar activity compared to solar  
 220 cycle 23. Also, according to the work of [13], which, analyzing the storm of December 5 and 6, 2010 in  
 221 New Brunswick found heavy precipitation and a storm surge that caused flooding. This coincided with  
 222 the arrival of a high-speed HSS/CIR flow with dense high-density plasma at its leading edge on 6  
 223 December. According to the work of [35]; [36], CIRs play a dominant role as a source of geomagnetic  
 224 disturbances during the solar minimum. Indeed, as the Sun rotates, high-speed fluxes (HSS) emitted  
 225 from coronal holes can interact with ambient slow solar wind fluxes, compressing the plasma at the  
 226 boundary, increasing the density in the region of slow solar wind. If the configuration of the solar corona  
 227 is stable, the pattern of interaction regions repeats with each rotation of the Sun, and they are called  
 228 corotating interaction regions [37], [38]. In the fast solar wind, the kinetic energy of the plasma is  
 229 converted into thermal energy, resulting in heating of the plasma and a decrease in density [38]. During  
 230 this interaction of fast solar winds and slow solar winds the plasma becomes very dense and very hot  
 231 and contributes to heating the convective clouds, increasing precipitation. We can therefore say that  
 232 solar activity is one of the many factors that affect climatic conditions, in particular precipitation.



233  
 234 Figure 5: Profile of precipitation and the solar wind energy during the period 1984 to 2022.

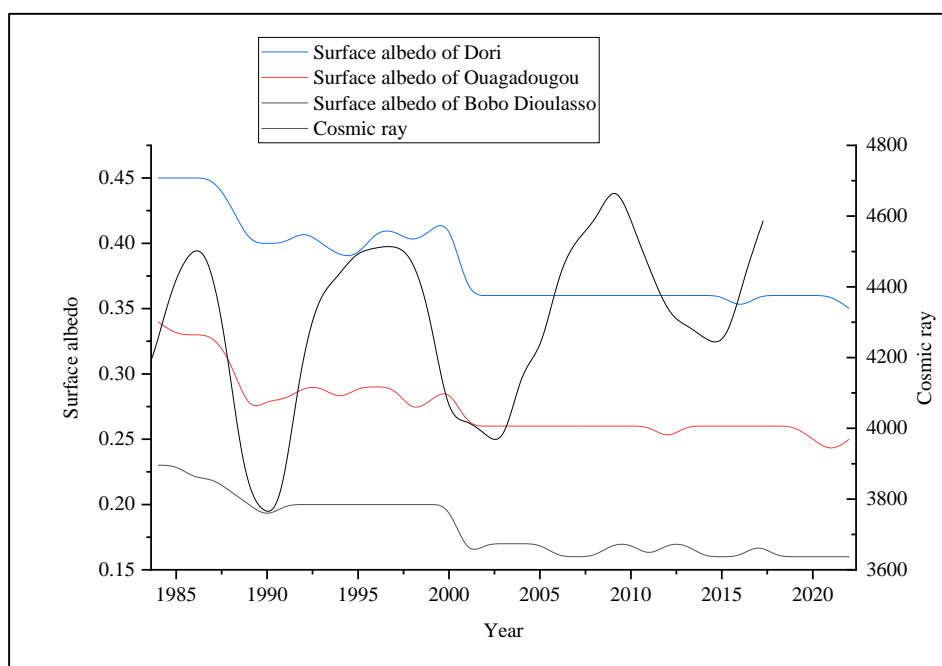
235 Figure 6, presents the temporal evolution profiles of the sunspot number and the surface albedo of Bobo  
 236 Dioulasso, Ouagadougou and Dori during the period 1984 to 2022. The two parameters studied present  
 237 a weak correlation. However, we can notice that the abrupt decreases in albedo are observed at the  
 238 maximum phase of each solar cycle. We also observe a constant evolution of the albedo after the solar  
 239 minimum of solar cycle 23, with slight fluctuations in 2011 and 2017 in Bobo-Dioulasso, in 2016 in  
 240 Ouagadougou and in 2012 and 2021 in Dori. According to [39], the Sun is, on average, more irradiating  
 241 at maximum activity than at a minimum of its cycle activity approximately 11 years. Also according to  
 242 [40], the variation in magnetic activity during the course of the 11-year cycle influences not only the  
 243 sunspot number and the magnetic flux but also the radiation emitted by the Sun and which we receive  
 244 on Earth called total or “constant” solar irradiance. [41] showed that the total irradiance varies in phase  
 245 with the solar cycle by about 0.1%: the higher the sunspot number, the higher the flux we receive from  
 246 the Sun, due to of the massive presence of faculae which are brighter zones. Furthermore, during the  
 247 solar maximum, coronal mass ejections are the most important events and dissipate a large amount of  
 248 energy in the interplanetary medium [14]. Thus, we can say that the Earth receives a large amount of  
 249 energy during the solar maximum compared to other phases of the solar cycle. This can lead to a  
 250 reduction in surface albedo. This is clearly observed in 1989 and 1990 at solar cycle 22 and in 2001 at  
 251 solar cycle 23, where an sudden decrease in albedo was recorded.



252  
 253 Figure 6: Profiles of the sunspot number and the surface albedo during the period 1984-2022.

254 Figure 7, presents the cosmic ray and albedo profiles of Bobo-Dioulasso, Ouagadougou and Dori during  
 255 the period 1984 to 2022. The two profiles show a weak correlation, but however the lowest cosmic ray  
 256 values are accompanied by a sudden decrease in albedo. We can also note that the amplitudes of  
 257 cosmic rays are significant over the last decade (2005-2022), with an almost linear evolution of the  
 258 albedo. This is explained by the low solar activity observed during this period. According to the work of  
 259 (Kakad et al., 2019[33], Somaila et al., 2022[34]), the solar activity of solar cycle 24 has been weak  
 260 compared to solar cycle 23, and is also manifested in the solar magnetic field. Furthermore, according

261 to the same authors, the calm Sun causes significant cloud cover while the active Sun induces less  
 262 cloud cover. [42] claims that the magnetic field of the solar wind influences the cosmic rays responsible  
 263 for the formation of clouds.



264  
 265 **Figure 7: Cosmic ray and surface albedo profiles during the period 1984-2022.**  
 266 Thus, the solar minimum going hand in hand with an increase in cosmic radiation received by the Earth,  
 267 condensation would be made more efficient and the increase in cloud cover would be favored. Thus we  
 268 can say that intense solar activity releases a large quantity of energy onto Earth and a low rate of cosmic  
 269 rays. Which leads to a drop in albedo, low cloud cover, and fluctuating temperatures. Low solar activity  
 270 leads to a high rate of cosmic rays in the interplanetary medium and this leads to significant cloud cover.  
 271 Thus part of the solar energy would be absorbed by this cloud cover, and would have less impact on  
 272 the surface albedo.

273 **4. Conclusion**

274 In this study, we examined solar flux and climatic parameters in three cities in Burkina Faso, located in  
 275 three different climatic zones. This study reveals a continued decrease in albedo in Burkina Faso leading  
 276 to significant global warming. This global warming causes an increase in temperature, specific humidity  
 277 and precipitation, increasing the risks of severe droughts and floods. This decline in albedo can be  
 278 explained by increasing urbanization, deforestation, manifestations of solar activity and global climate  
 279 change. Heavy precipitation is observed during periods of low solar activity and also during high-speed  
 280 flow events caused by regions of co-rotating interactions. The continued decrease in albedo can be  
 281 mitigated by favoring more reflective construction materials, i.e. high albedo, and stopping the  
 282 transformation of forests into cultivatable land.

283

293 **References**

- 294 1. Guo, T., He, T., Liang, S., Roujean, J.-L., Zhou, Y., Huang, X., 2022. Multi-decadal analysis of high-  
295 resolution albedo changes induced by urbanization over contrasted Chinese cities based on  
296 Landsat data. *Remote Sens. Environ.* 269, 112832. <https://doi.org/10.1016/j.rse.2021.112832>
- 297 2. Santos Orozco, D.L., Ruiz Corral, J.A., Villavicencio García, R.F., Rodríguez Moreno, V.M., 2023.  
298 Deforestation and Its Effect on Surface Albedo and Weather Patterns. *Sustainability* 15,  
299 11531. <https://doi.org/10.3390/su151511531>
- 300 3. Hu, Y., Hou, M., Zhao, C., Zhen, X., Yao, L., Xu, Y., 2019. Human-induced changes of surface  
301 albedo in Northern China from 1992-2012. *Int. J. Appl. Earth Obs. Geoinformation* 79, 184–191.  
302 <https://doi.org/10.1016/j.jag.2019.03.018>
- 303 4. He, T., Wang, D., Qu, Y., 2018. Land surface albedo.
- 304 5. Zhao, F., Lan, X., Li, W., Zhu, W., Li, T., 2021. Influence of Land Use Change on the Surface  
305 Albedo and Climate Change in the Qinling-Daba Mountains. *Sustainability* 13, 10153.  
306 <https://doi.org/10.3390/su131810153>
- 307 6. Bhattacharya, B., Gunjal, K., Panigrahy, S., Parihar, J., 2011. Albedo-rainfall Feedback Over Indian  
308 Monsoon Region Using Long Term Observations Between 1981 to 2000. *J. Indian Soc. Remote Sens.*  
309 39, 393–406. <https://doi.org/10.1007/s12524-011-0136-9>
- 310 7. Charney, J., Quirk, W., Chow, S., Kornfield, J., 1977. A Comparative Study of the Effects of Albedo  
311 Change on Drought in Semi-Arid Regions. *J. Atmospheric Sci.* 34.  
312 [https://doi.org/10.1175/1520-0469\(1977\)034<1366:ACSOTE>2.0.CO;2](https://doi.org/10.1175/1520-0469(1977)034<1366:ACSOTE>2.0.CO;2)
- 313 8. Fuller, D.O., Ottke, C., 2002. Land Cover, Rainfall and Land-Surface Albedo in West Africa. *Clim.*  
314 *Change* 54, 181–204. <https://doi.org/10.1023/A:1015730900622>
- 315 9. Govaerts, Y., Lattanzio, A., 2008. Estimation of surface albedo increase during the eighties Sahel  
316 drought from Meteosat observations. *Glob. Planet. Change* 64.  
317 <https://doi.org/10.1016/j.gloplacha.2008.04.004>
- 318 10. Andrés-Anaya, P., Sánchez-Aparicio, M., del Pozo, S., Lagüela, S., 2021. Correlation of Land  
319 Surface Temperature with IR Albedo for the Analysis of Urban Heat Island. *Eng. Proc.* 8, 9.  
320 <https://doi.org/10.3390/engproc2021008009>

- 321 11. Lopez-Cabeza, V.P., Alzate-Gaviria, S., Diz-Mellado, E., Rivera-Gomez, C., Galan-Marin, C.,  
322 2022. Albedo influence on the microclimate and thermal comfort of courtyards under  
323 Mediterranean hot summer climate conditions. *Sustain. Cities Soc.* 81, 103872.  
324 <https://doi.org/10.1016/j.scs.2022.103872>
- 325 12. Doughty, C.E., Loarie, S.R., Field, C.B., 2012. Theoretical Impact of Changing Albedo on  
326 Precipitation at the Southernmost Boundary of the ITCZ in South America. *Earth Interact.* 16,  
327 1–14. <https://doi.org/10.1175/2012EI422.1>
- 328 13. Prikryl, P., Rušin, V., 2023. Occurrence of heavy precipitation influenced by solar wind high-speed  
329 streams through vertical atmospheric coupling. *Front. Astron. Space Sci.* 10.
- 330 14. Sawadogo, Y., Koala, S., Zerbo, J.L., 2022. Rainfall and Temperature Variations over Burkina  
331 Faso: Possible Influence of Geomagnetic Activity, Solar Activity and Associated Energies from  
332 1975 to 2020. *Atmospheric Clim. Sci.* 12, 603–612. <https://doi.org/10.4236/acs.2022.124034>
- 333 15. Allen, M.R., Ingram, W.J., 2002. Constraints on future changes in climate and the hydrologic cycle.  
334 *Nature* 419, 224–232. <https://doi.org/10.1038/nature01092>
- 335 16. O’Gorman, P.A., Muller, C.J., 2010. How closely do changes in surface and column water vapor  
336 follow Clausius–Clapeyron scaling in climate change simulations? *Environ. Res. Lett.* 5,  
337 025207.
- 338 17. Bao, J., Sherwood, S.C., Alexander, L.V., Evans, J.P., 2017. Future increases in extreme  
339 precipitation exceed observed scaling rates. *Nat. Clim. Change* 7, 128–132.  
340 <https://doi.org/10.1038/nclimate3201>
- 341 18. Changnon, S.A., Kunkel, K.E., Reinke, B.C., 1996. Impacts and Responses to the 1995 Heat  
342 Wave: A Call to Action. *Bull. Am. Meteorol. Soc.* 77, 1497–1506. [https://doi.org/10.1175/1520-0477\(1996\)077<1497:IARTTH>2.0.CO;2](https://doi.org/10.1175/1520-0477(1996)077<1497:IARTTH>2.0.CO;2)
- 344 19. Anderson, B.G., Bell, M.L., 2009. Weather-Related Mortality. *Epidemiol. Camb. Mass* 20, 205–  
345 213. <https://doi.org/10.1097/EDE.0b013e318190ee08>
- 346 20. Kalkstein, L.S., Greene, S., Mills, D.M., Samenow, J., 2011. An evaluation of the progress in  
347 reducing heat-related human mortality in major U.S. cities. *Nat. Hazards* 56, 113–129.  
348 <https://doi.org/10.1007/s11069-010-9552-3>
- 349 21. Kalkstein, L.S., Sailor, D., Shickman, K., Sheridan, S., Vanos, J., 2013. Assessing the health  
350 impacts of urban heat island reduction strategies in the District of Columbia. Rep. DDOE ID.
- 351 22. Vanos, J.K., Kalkstein, L.S., Sanford, T.J., 2015. Detecting synoptic warming trends across the US  
352 Midwest and implications to human health and heat-related mortality. *Int. J. Climatol.* 35, 85–  
353 96. <https://doi.org/10.1002/joc.3964>
- 354 23. McGugan, E.A., 2001. Hyperpyrexia in the emergency department. *Emerg. Med.* 13, 116–120.  
355 <https://doi.org/10.1046/j.1442-2026.2001.00189.x>
- 356 24. Matsoukis, A., Kamoutsis, A., Bollas, A., Chronopoulou-Sereli, A., 2013. Biometeorological  
357 Conditions in the Urban Park of Nea Smirni in the Greater Region of Athens, Greece During  
358 Summer, in: Helmis, C.G., Nastos, P.T. (Eds.), *Advances in Meteorology, Climatology and*  
359 *Atmospheric Physics*, Springer Atmospheric Sciences. Springer, Berlin, Heidelberg, pp. 217–  
360 222. [https://doi.org/10.1007/978-3-642-29172-2\\_31](https://doi.org/10.1007/978-3-642-29172-2_31)

- 361 25. Qiu, G., Li, H., Zhang, Q., Chen, W., Liang, X., Li, X., 2013. Effects of Evapotranspiration on  
362 Mitigation of Urban Temperature by Vegetation and Urban Agriculture. *J. Integr. Agric.* 12,  
363 1307–1315. [https://doi.org/10.1016/S2095-3119\(13\)60543-2](https://doi.org/10.1016/S2095-3119(13)60543-2)
- 364 26. Dickinson, R.E., Henderson-Sellers, A., 1988. Modelling tropical deforestation: A study of GCM  
365 land-surface parametrizations. *Q. J. R. Meteorol. Soc.* 114, 439–462.  
366 <https://doi.org/10.1002/qj.49711448009>
- 367 27. D’Almeida, C., Vörösmarty, C.J., Hurtt, G.C., Marengo, J.A., Dingman, S.L., Keim, B.D., 2007. The  
368 effects of deforestation on the hydrological cycle in Amazonia: a review on scale and  
369 resolution. *Int. J. Climatol.* 27, 633–647. <https://doi.org/10.1002/joc.1475>
- 370 28. Ouyang, Z., Sciusco, P., Jiao, T., Feron, S., Lei, C., Li, F., John, R., Fan, P., Li, X., Williams, C.A.,  
371 Chen, G., Wang, C., Chen, J., 2022. Albedo changes caused by future urbanization contribute  
372 to global warming. *Nat. Commun.* 13, 3800. <https://doi.org/10.1038/s41467-022-31558-z>
- 373 29. Canadell, J.G., Raupach, M.R., 2008. Managing Forests for Climate Change Mitigation. *Science*  
374 320, 1456–1457. <https://doi.org/10.1126/science.1155458>
- 375 30. Jin, M., Dickinson, R.E., Zhang, D., 2005. The Footprint of Urban Areas on Global Climate as  
376 Characterized by MODIS. *J. Clim.* 18, 1551–1565. <https://doi.org/10.1175/JCLI3334.1>
- 377 31. Legrand, J., Simon, P., 1989. Solar cycle and geomagnetic activity: A review for geophysicists.  
378 Part I. The contributions to geomagnetic activity. *Ann Geophys* 7, 565–578.
- 379 32. Zerbo, J.-L., Ouattara, F.M., Amory-Mazaudier, C., Legrand, J.-P., Richardson, J.D., 2013. Solar  
380 Activity, Solar Wind and Geomagnetic Signatures. *Atmospheric Clim. Sci.* 3, 610.  
381 <https://doi.org/10.4236/acs.2013.34063>
- 382 33. Kakad, B., Kakad, A., Ramesh, D.S., Lakhina, G.S., 2019. Diminishing activity of recent solar  
383 cycles (22–24) and their impact on geospace. *J. Space Weather Space Clim.* 9, A1.  
384 <https://doi.org/10.1051/swsc/2018048>
- 385 34. Somaïla, K., Yacouba, S., Louis, Z.J., 2022. Solar wind and geomagnetic activity during two  
386 antagonist solar cycles: Comparative study between the solar cycles 23 and 24. *Int. J. Phys.*  
387 *Sci.* 17, 57–66. <https://doi.org/10.5897/IJPS2022.4998>
- 388 35. Gonzalez, W.D., Tsurutani, B.T., Clúa de Gonzalez, A.L., 1999. Interplanetary origin of  
389 geomagnetic storms. *Space Sci. Rev.* 88, 529–562. <https://doi.org/10.1023/A:1005160129098>
- 390 36. Tsurutani, B.T., Gonzalez, W.D., Gonzalez, A.L.C., Tang, F., Arballo, J.K., Okada, M., 1995.  
391 Interplanetary origin of geomagnetic activity in the declining phase of the solar cycle. *J.*  
392 *Geophys. Res. Space Phys.* 100, 21717–21733. <https://doi.org/10.1029/95JA01476>
- 393 37. Smith, E.J., Wolfe, J.H., 1976. Observations of interaction regions and corotating shocks between  
394 one and five AU: Pioneers 10 and 11. *Geophys. Res. Lett.* 3, 137–140.  
395 <https://doi.org/10.1029/GL003i003p00137>
- 396 38. Echer, E., Gonzalez, W.D., Alves, M.V., 2006. On the geomagnetic effects of solar wind  
397 interplanetary magnetic structures. *Space Weather* 4. <https://doi.org/10.1029/2005SW000200>
- 398 39. Kopp, G., Lean, J.L., 2011. A new, lower value of total solar irradiance: Evidence and climate  
399 significance. *Geophys. Res. Lett.* 38. <https://doi.org/10.1029/2010GL045777>
- 400 40. Bard, E., Frank, M., 2006. Climate change and solar variability: What’s new under the Sun. *epsl*

- 401           248, 1. <https://doi.org/10.1016/j.epsl.2006.06.016>
- 402 41. Lean, J., Rottman, Gary, Harder, J., Kopp, G., 2005. *SORCE Contributions to New Understanding*
- 403           of Global Change and Solar Variability, in: Rottman, G., Woods, T., George, V. (Eds.), *The*
- 404           Solar Radiation and Climate Experiment (SORCE): Mission Description and Early Results.
- 405           Springer, New York, NY, pp. 27–53. [https://doi.org/10.1007/0-387-37625-9\\_3](https://doi.org/10.1007/0-387-37625-9_3)
- 406 42. Svensmark, H., 1998. Influence of Cosmic Rays on Earth's Climate. *Phys. Rev. Lett.* 81, 5027–
- 407           5030. <https://doi.org/10.1103/PhysRevLett.81.5027>
- 408